Bioorganic Chemistry 105 (2020) 104403

Contents lists available at ScienceDirect

Bioorganic Chemistry

journal homepage: www.elsevier.com/locate/bioorg

An allomaltol derivative triggers distinct death pathways in luminal a and triple-negative breast cancer subtypes

A. Ercan [a], S. Oncul [a], G. Karakaya [b], M. Aytemir [b,c,*]

[a] Hacettepe University, Faculty of Pharmacy, Department of Biochemistry, Ankara, Turkey
[b] Izmir Katip Çelebi University, Faculty of Pharmacy, Department of Pharmaceutical Chemistry, Izmir, Turkey
[c] Hacettepe University, Faculty of Pharmacy, Department of Pharmaceutical Chemistry, Ankara, Turkey

ARTICLE INFO

Keywords:
Breast cancer
Kojic acid
Allomaltol
Apoptosis
Multidrug resistance

ABSTRACT

Breast cancer is the most common cancer in women that shows a predisposition to metastasize to the distant organs. Kojic acid is a natural fungal metabolite exhibiting various biological activities. Compounds derived from kojic acid have been extensively studied and proved to demonstrate anti-neoplastic features on different cancer types. In the present study, allomaltol-structural analog of kojic acid and its seven derivatives including four novel compounds, have been synthesized, characterized and their possible impact on breast cancer cell viability was investigated. It was discovered that compound 5, bearing 3,4-dichlorobenzyl piperazine moiety, could decrease the viability of both MCF-7 and MDA-MB-231 cell lines distinctively. To ascertain the death mechanism, cells were subjected to different tests following the application of IC_{50} concentration of compound 5. Data obtained from lactate dehydrogenase activity and gene expression assays pointed out that necrosis had taken place predominantly in MDA-MB-231. On the other hand, in MCF-7 cells, the p53 apoptotic pathway was activated by overexpression of the pro-apoptotic TP53 and Bax genes and suppression of the anti-apoptotic Mdm-2 and Bcl-2 genes. Furthermore, Bax/Blc-2 ratio was escalated by 3.5 fold in the study group compared to the control. Compound 5 did not provoke drug resistance in MCF-7 cells since the Mdr-1 gene expression, drug efflux, and H_2O_2 content remained unaltered. As for MDA-MB-231 cells, only a 1.4 fold increase in the Mdr-1 gene expression was detected. These results indicate the advantage of the allomaltol derivative over the chemotherapeutic agents conventionally used for breast cancer treatment that can be highly toxic and mostly lead to drug resistance. Thus, this specific allomaltol derivative offers an alternative therapeutic approach for breast cancer which needs further investigation.

1. Introduction

Breast cancer is the second leading cause of death from cancer among women worldwide [1]. Treatment options for breast cancer comprise surgical debulking, radiation, chemotherapy, hormone therapy, and targeted therapies. To design an effective treatment strategy, it is essential to determine the specific features of the cancer cells such as possession of receptors like progesterone receptor (PR), estrogen receptor (ER) and human epidermal growth factor receptor 2 (HER2), drug resistance potential and response to chemotherapy [2]. Chemotherapy is the main approach to target the rapid and uncontrolled tumor cell proliferation regardless of the subtype of cancer cells. However, the hereditary or acquired multiple drug resistance (MDR) where the cells become resistant to a chemotherapeutic agent(s), particularly due to overexpression of certain transmembrane proteins such as adenosine triphosphate (ATP) binding cassette (ABC) transporter family members limit their expediency [3,4]. Therefore, numerous studies have been conducted to overcome chemotherapy-related MDR while targeting cancer cells selectively.

5-Hydroxy-2-(hydroxymethyl)-4*H*-pyran-4-one (Kojic acid, KA) is a natural secondary metabolite produced by certain *Aspergillus*, *Acetobacter*, and *Penicillium* species. It is a potent tyrosinase inhibitor, therefore capable of suppressing melanogenesis as the first and the rate-limiting step of melanogenesis that is catalyzed by tyrosinase enzyme [5,6]. It is used as a food additive to prevent enzymatic discoloration as well as in the cosmetic industry to alleviate hyperpigmentation of the skin by its tyrosinase inhibition property caused primarily by sunburn, UV light, and scars [7,8]. KA is also proven to exhibit anti-inflammatory,

* Corresponding author at: Hacettepe University, Faculty of Pharmacy, Department of Pharmaceutical Chemistry, 06100 Sihhiye - Ankara, Turkey.
E-mail address: mutlud@hacettepe.edu.tr (M. Aytemir).

https://doi.org/10.1016/j.bioorg.2020.104403
Received 26 July 2020; Received in revised form 24 September 2020; Accepted 18 October 2020
Available online 21 October 2020

anti-bacterial, and anti-neoplastic activities [9,10]. Due to its instability during long term storage as well as its capacity to provoke skin irritation in high concentrations, studies have focused on synthesizing KA derivatives with less harmful effects [11–15].

2-Chloromethyl-5-hydroxy-4*H*-pyran-4-one (chlorokojic acid, CKA) and 5-hydroxy-2-methyl-4*H*-pyran-4-one (allomaltol, ALM) are structural analogs of KA and can be synthesized from commercially available KA [8]. ALM and its derivatives draw attention due to their advantageous activities including anticancer [16], antidiabetic [17] and antimalarial [18].

Mannich bases that are derivatives of the KA scaffold were shown to suppress inflammation, infection, and cancer cell proliferation [8,12]. Recently, we have reported the synthesis of new KA derivatives and examined their cytotoxic effects on A375 human malignant melanoma, HGF-1 human gingival fibroblasts, and MRC-5 human lung cell lines [15,19]. We have found that most of the compounds were not harmful to the healthy cell lines while representing cytotoxic action on cancerous A375 cells significantly higher than the drugs used for the treatment of malignant melanoma such as dacarbazine, temozolomide, and lenalidomide. Especially, compounds bearing 3,4-dichlorobenzyl piperazine moiety which one is also included in the context of this study as an ALM derivative showed greater inhibition against A375 human malign melanoma cells compared to the reference drugs [19].

Based on our previous studies [19,20] and as a part of our continuing interest in developing new anticancer agents, we reported the synthesis of seven ALM derivatives having a structure of 2-substituted-6-methyl-3-hydroxy-4*H*-pyran-4-one, using the methodology shown in Fig. 1. In this study, we explored the contribution of the compounds on the viability of MCF-7 and MDA-MB-231 breast cancer cell lines for the first time. After stating the most effective compound, the mechanism of the cell death and the drug resistance were studied. Data for the synthesis of the effective compound and its activity on A375 malignant melanoma cell line have already been established [19] and have been applied to the Turkish Patent and Trademark Office (TR2017/20155). Physical properties of the compounds including their molecular formula, yields, and melting points are given in Table 1.

2. Results

2.1. Chemistry

3-Hydroxy-4*H*-pyran-4-ones comprising KA, CKA, and ALM are important classes of the structural motif of many compounds both natural and synthetic, possessing high biological activity profile. Therefore, their synthesis is of great importance to medicinal chemists, and studies have been ongoing for years to come up with more effective and safer agents. CKA and ALM have a structure very close to that of KA wherein the hydroxymethyl group is replaced with the chloromethyl and methyl groups, respectively. As the chlorine in the structure of CKA readily undergoes nucleophilic substitution, it is a crucial compound from the chemical point of view. ALM has also been reported to be a non-toxic and potential ligand for the chelation of metals [17]. CKA is produced at room temperature via chlorination of the 2-hydroxymethyl moiety of KA by thionyl chloride, with the ring hydroxyl being unaffected. Later CKA is reduced to ALM harnessing zinc dust in concentrated hydrochloric acid [8].

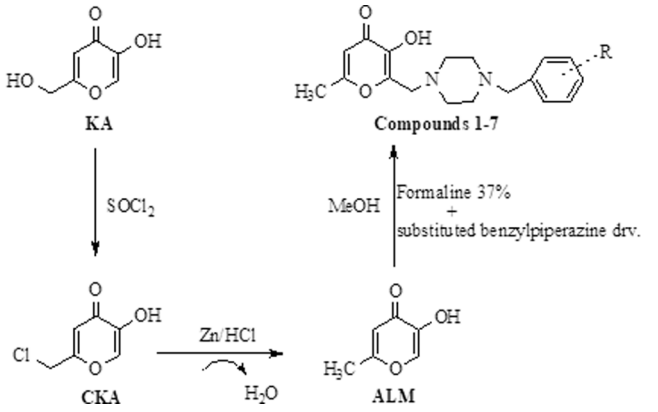

Fig. 1. The basic synthesis process of the ALM derivatives.

The one-pot Mannich reaction of ALM with appropriately substituted benzylpiperazine derivatives in the presence of formalin occurred with good yields. Because of phenol-like properties, aminomethylation *ortho* to the enolic hydroxyl group was constructed in a short time. The mechanism of this reaction relies on the enhanced activity in the basic medium due to increased electronegativity at the 6th position of the hydroxypyrone ring [21]. The resulting precipitate as Mannich bases was collected by filtration and washed with cold methanol.

The characterization of the novel compounds was supported by FT-IR, MS, ^{1}H, and ^{13}C NMR spectroscopy techniques and the elemental analysis data. The selected diagnostic bands of IR spectra of the compounds provide useful information to determine the structures in terms of absorption bands that are about 1620 cm^{-1} due to (C═O) stretching of the pyranone ring. The assignment of the signals from the ^{1}H NMR spectra was based on the chemical shifts and intensity pattern. The singlet peaks owing to –CH_3 group at the 6th position of the pyrone ring exhibited signals between 2.24 and 2.41 ppm. The spectrums showed broad singlet peaks for -CH_2- of piperazine between 2.39 and 2.62 ppm. The aromatic protons of the phenyl rings appeared in the range of 7.20 and 7.53 ppm. Characteristic H^5 proton of the 4*H*-pyran-4-one ring was determined as singlet peaks at about 6.5 ppm. The ^{13}C NMR signals of the compounds were in accordance with the proposed structures. Carbonyl carbons of the 4*H*-pyran-4-one ring were found around 173 ppm. The distinctive signals of compounds were observed in the mass spectra which followed a similar fragmentation pattern. The entire spectrums showed characteristic molecular ion peaks equivalent to their molecular formulae, M^++23 (Na) peaks, and M^++1 isotope peaks owing to chlorine and bromine atoms with the ratio of 1:1 and 3:1, respectively.

2.2. Biological screening

Compounds synthesized in this study (Table 1, Fig. 1) were screened for their *in vitro* cytotoxic activities against breast cancer cell lines MCF-7 and MDA-MB-231 using sulforhodamine B (SRB) assay upon 24, 48, or 72 h of exposure. ALM and its seven derivatives were tested, where all compounds of this subset had weak cytotoxicity against two breast cancer cell lines, except for **compound 5**. This compound has a 3,4-dichloro group at R position and showed the highest toxicity on MCF-7 (96.95 μM) and MDA-MB-231 (47.79 μM) at 48 h. The cytotoxic activity of the compound was evaluated against the human gingival fibroblast cell line (HGF-1) as a representative of normal (non-cancerous) cells and was found to be 410.4 μM (data not shown). The *in vitro* cytotoxic selectivity of **compound 5** on the HGF-1 cell line was used to detect the selectivity index (SI), by the equation stated as follows:

$$SI = IC_{50}^{\text{non-cancerous cell line}} / IC_{50}^{\text{cancer cell line}}$$

The selectivity index for MCF-7 and MDA-MB-231 cell lines were calculated to be 4.2 and 8.6, respectively. This compound was harmless over non-cancerous HGF-1 but was cytotoxic on both of the breast cancer cell lines. To highlight the advantage of **compound 5**, we compared its SI values with Doxorubicin (DOX), which is widely used in the treatment regimens of breast cancer. Being a very potent chemotherapy agent, DOX binds to the DNA, disturbs membrane permeability, and generates a large amount of reactive oxygen species (ROS) [22]. However, DOX is known to be very toxic on non-cancerous cells as well

Table 1
Physicochemical properties of the compounds 1–7.

Comp.	Structure	Molecular formula	Molecular weight (g/mol)	Yield	M.p. (°C)
	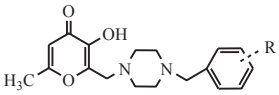				
	R				
1[a]	4-fluoro	$C_{18}H_{21}FN_2O_3$	332.37	66	168–70
2	4-trifluoromethyl	$C_{19}H_{21}F_3N_2O_3$	382.38	71	171–2
3[a]	2,5-difluoro	$C_{18}H_{20}F_2N_2O_3$	350.36	70	163–5
4	2,6-dichloro	$C_{18}H_{20}Cl_2N_2O_3$	383.27	60	165–6
5[b]	3,4-dichloro	$C_{18}H_{20}Cl_2N_2O_3$	383.27	60	160–2
6	2-chloro-6-fluoro	$C_{18}H_{20}ClFN_2O_3$	366.81	20	153–5
7	4-bromo-2-fluoro	$C_{18}H_{20}BrFN_2O_3$	411.27	47	180–1
ALM		$C_6H_6O_3$	126.11	63	153–5

[a] : [20].
[b] :[19].

and is associated with congestive heart failure and cardiomyopathy [23]. Therefore, the search for a compound that exerts no/less cytotoxicity over non-cancerous cells is crucial at this point. The IC_{50} values of DOX at 48 h for MCF-7 and MDA-MB-231 were detected previously by our team to be 8.3 μM and 6.6 μM, respectively [24]. The non-cancerous cell line to be tested for DOX was chosen to be HEK293 and IC_{50} was calculated as 0.37 μM. The SI values for DOX in MCF-7 and MDA-MB-231 were 0.044 and 0.056, respectively. These data indicate that although DOX is very effectively used in breast cancer cell treatment, its cytotoxic effect on non-cancerous cells is intimidating. **Compound 5**, therefore is effective in breast cancer cell lines MCF-7 and MDA-MB-231 and safe for the non-cancerous cells.

The novel Mannich Base derivative that showed the highest cytotoxicity and SI value (**compound 5**) was tested for further *in vitro* experiments to explore the mechanism of cell death. IC_{50} concentrations of the compound at 48 h for each cell line were given in Table 2. Dose-dependent changes in the proliferation of MCF-7 and MDA-MB-231 cells exposed to **compound 5** for 24, 48, or 72 h were shown in Fig. 2.

2.3. Assessment of the stability of compound 5

The UV–visible absorption spectrum of **compound 5** was measured at three time-points (0 h, 24 h, 48 h) and the maximum absorbance of the derivative was determined to be 246–262 nm and within the UV range. **Compound 5** was proved to be stable for at least 48 h at 37 °C since the optical properties of the ALM derivative were intact throughout the measurement schedule. The graphic regarding the maximum absorbance and the stability over time was given in Fig. 3.

Table 2
IC_{50} values of ALM and compounds 1–7 for MCF-7 and MDA-MB-231 breast cancer cell lines (n = 3 ± SD).

Compounds	IC_{50} (μM)	
	MCF-7	**MDA-MB-231**
ALM	396.4	358.6
1	424	155.6
2	105	42.48
3	234.4	416.9
4	150.7	122.5
5	**96.95**	**47.79**
6	204.4	159.1
7	182.1	145.5

2.4. ALM derivative-induced lactate dehydrogenase (LDH) leakage

Toxicity rates of the IC_{50} values (of 48 h) of **compound 5** were also examined in terms of LDH leakage from the cells, which is an assessment of cellular membrane integrity, and hence a marker for necrotic cell death. The percentages of the cytotoxicity based on LDH leakage were calculated abiding by the equation given in the materials and methods section. It was witnessed that the LDH activity in the media of both of the cells was increased significantly when the caspase inhibitor Z-VAD-FMK was applied to the breast cancer cells alone or in combination with **compound 5** for 6 h. LDH activity remained unchanged with the treatment of MCF-7 cells with **compound 5** (**A**) although; the activity was increased by ~ 30% when MDA-MB-231 cells were exposed to the derivative (**B**) (Fig. 4). These results indicated that the treatment schedule with **compound 5** led MDA-MB-231 cells to necrosis meanwhile, it triggered a programmed cell death mechanism in MCF-7 cells.

2.5. Measurement of hydrogen peroxide (H_2O_2) level

Changes in H_2O_2 intracellular concentrations cause responses that vary greatly but they frequently lead to cell death. Thus, the internal H_2O_2 level upon administration of **compound 5** was investigated to understand whether a ROS and mitochondria-based cell death mechanism takes place or not. Based on the data of 48 h, the H_2O_2 level was observed to be attenuated distinctly in MCF-7 cells when exposed to the compound, compared to the control. In opposite, H_2O_2 production was detected to be slightly increased in MDA-MB-231 upon treatment (Fig. 5). Taking into consideration cell cytotoxicity and LDH leakage experiments, this can be explained by that **compound 5** surprisingly does not generate intracellular H_2O_2 in MCF-7 cells. Moreover, the compound suppressed the internal ROS production meanwhile exerting its cytotoxic effect on the cell. The slight stimulation of the H_2O_2 production in MDA-MB-231 cells can be attributed to the increased sensitivity of the cells to metabolites such as reactive nitrogen species (NOS) which is a hypothesis that needs to be confirmed in the future studies.

2.6. Alterations in caspase 8 and 9 activity upon treatment of the cells with compound 5

Following the assessments of cytotoxicity, LDH leakage, and H_2O_2 generation; caspase activity was investigated to determine whether the compound triggers the breast cancer cell lines to undergo apoptosis. According to the results, the activity of caspases 8 and 9 was provoked

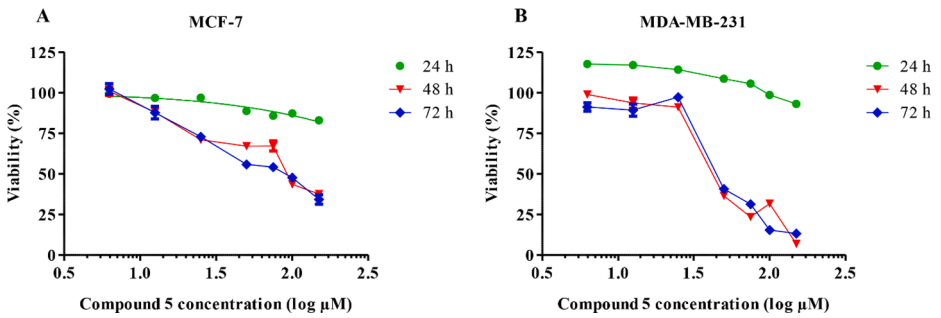

Fig. 2. The evaluation of the cytotoxic effect of **compound 5** on **(A)** MCF-7 and **(B)** MDA-MB-231 cells at 24, 48, or 48 h (n = 3 ± SD).

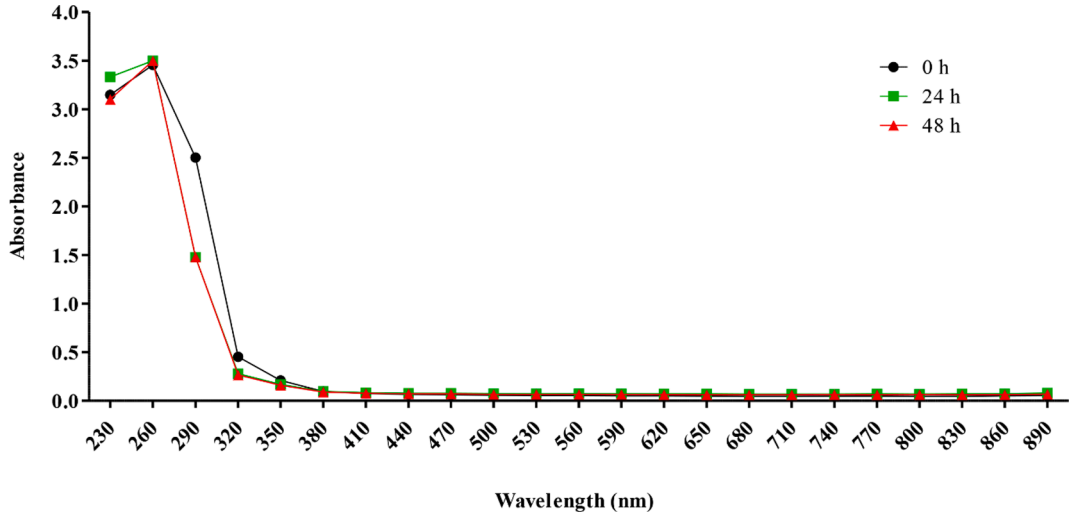

Fig. 3. UV–visible spectra of the ALM derivative, **compound 5** at 0 h, 24 h, and 48 h. The maximum absorbance of **compound 5** was measured to be 246–262 nm and the molecule was stable for at least 48 h at 37 °C.

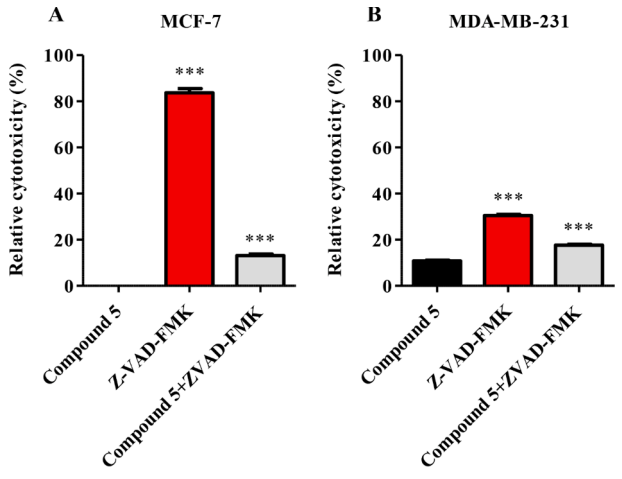

Fig. 4. The relative toxicity of **(A)** MCF-7 and **(B)** MDA-MB-231 cells exposed to the IC_{50} concentration (48 h) of **compound 5**. The cells were treated with compound 5, Z-VAD-FMK, or both for 6 h to examine the LDH activity in media (n = 3 ± SD; ***p < 0.001 vs. compound 5).

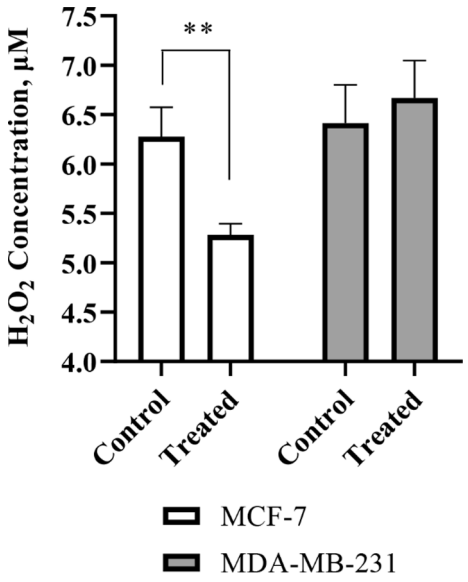

Fig. 5. The concentration of H_2O_2 released to the medium from MCF-7 and MDA-MB-231 treated with IC_{50} dosage of **compound 5** for 48 h (n = 3 ± SD; **p < 0.01).

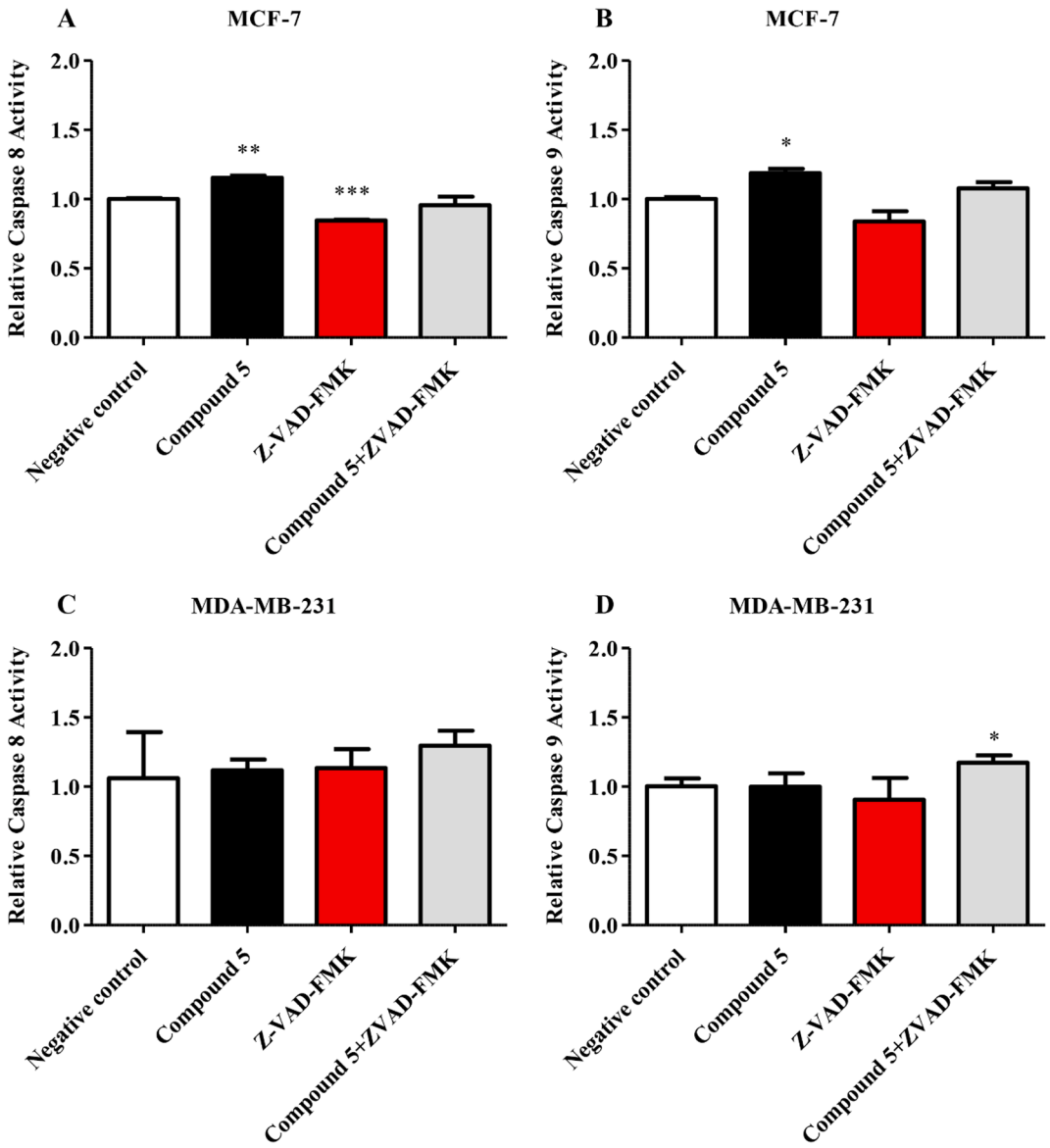

Fig. 6. The caspase 8 and 9 activity levels in **(A** and **B)** MCF-7 and **(C** and **D)** MDA-MB-231 cells following the incubation of the cells with **compound 5** for 6 h. **(A** and **B)** Caspase 8 and 9 activity rates were triggered with the subjection of MCF-7 cells to IC_{50} concentration (for 48 h) of **compound 5**. Z-VAD-FMK inhibited the augmentation of the caspase 8 activity **(C** and **D)** The caspase levels did not differ in MDA-MB-231 cells when they were treated with the ALM derivative for 6 h ($n = 3 \pm SD$; *$p < 0.05$ vs. negative control, **$p < 0.01$, ***$p < 0.001$).

significantly with the incubation of MCF-7 cells with IC_{50} dosage (at 48 h) of **compound 5** for 6 h, indicating that apoptosis was triggered and the caspase inhibitor Z-VAD-FMK reversed the activation (Fig. 6 (**A** and **B**)). **Compound 5** application to MDA-MB-231 cells did not provoke the activity levels of caspase 8 or 9, which along with increased LDH activity point out to necrosis rather than apoptosis (Fig. 6 (**C** and **D**)).

2.7. Drug efflux from ALM derivative-treated cells

To investigate the role of **compound 5** on chemoresistance of MCF-7 and MDA-MB-231 cells, drug efflux was evaluated. In MCF-7 cells, calcein retention was noticed to be unaffected in comparison with the control, suggesting that **compound 5** faced the prolonged retention inside MCF-7 cells. Without being excluded from the cell, **compound 5** executed more of its cytotoxic damage in MCF-7 cells. On the other hand, the fluorescent signal of calcein slightly decreased in MDA-MB-231 treated with **compound 5** which may be attributed to necrosis the cells experienced**.** Graphics regarding the drug efflux assay results were given in Fig. 7.

2.8. Gene expression analysis

Quantitative real-time polymerase chain reaction (qRT-PCR) was carried out to identify expression levels of multidrug resistance gene Mdr-1 and particular genes of the apoptotic pathway. Upon subjection of MCF-7 cells to the IC_{50} concentration of compound 5, the pro-apoptotic TP53 gene was found to be overexpressed and the Bax/Bcl-2 ratio was highly upregulated. On the contrary, the p53-antagonist Mdm-2 gene was diminished (Fig. 8). Evaluating with previous findings, results indicated that compound 5 triggered the extrinsic apoptotic pathway by activating both caspase 8 and p53 gene and decreasing its negative regulator, Mdm-2. As MDA-MB-231 cells carry the mutant TP53 gene, the p53 apoptotic pathway is greatly impaired. In that case, all relevant genes assessed in this study were seen to be inhibited significantly (Fig. 9). Accordingly, MDA-MB-231 cell death was caspase-independent and clearly escaped from p53 regulation, pointing out a diverse cell

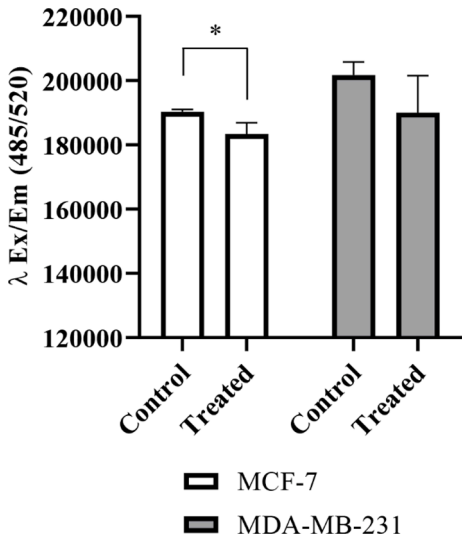

Fig. 7. Changes in calcein AM retention of MCF-7 and MDA-MB-231 cells after being subjected to the IC_{50} concentration of **compound 5** for 48 h (n = 3 ± SD; *p < 0.05).

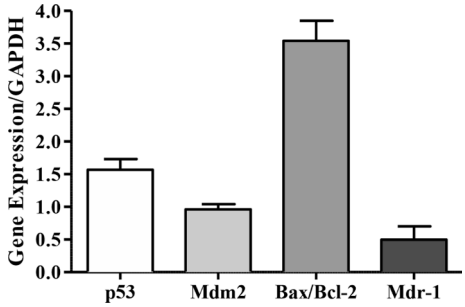

Fig. 8. Expression levels of pro-apoptotic (p53 and Bax), pro-survival (Mdm-2 and Bcl-2) and multidrug resistance (Mdr-1) genes compared to the control in MCF-7 cells in response to treatment with IC_{50} concentration of **compound 5** for 48 h (n = 3 ± SD).

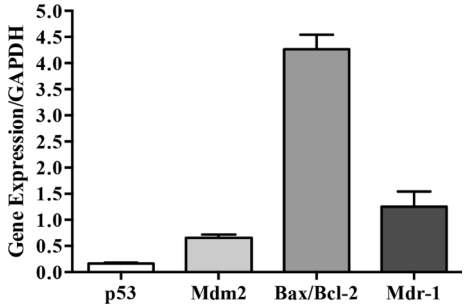

Fig. 9. **q**RT-PCR results for the pro-apoptotic (p53 and Bax), anti-apoptotic (Mdm-2 and Bcl-2), and multidrug resistance (Mdr-1) genes in MDA-MB-231 cells exposed to IC_{50} value of **compound 5** for 48 h. The expression levels were compared to the untreated control values and given as fold change (n = 3 ± SD; *p < 0.05, **p < 0.01, ***p < 0.001).

death mechanism other than apoptosis. Considering LDH activity and the highly metastatic characteristic of triple-negative breast cancer (TNBC) cell line MDA-MB-231, the results manifest necrosis. The Mdr-1 gene expression profiles of MCF-7 and MDA-MB-231 cells were consistent with the drug efflux assay data explained in Fig. 7. As can be seen in Fig. 8 and Fig. 9, Mdr-1 was inhibited in MCF-7 cells whilst it was activated in MDA-MB-231 cells. As explained previously, the suppression of the Mdr-1 gene was a surplus for the prolonged retention of compound 5 inside MCF-7 cells allowing the prolongation of the cytotoxic effect that led the cells to death. Similarly, the triggered Mdr-1 gene in MDA-MB-231 cells was consistent with the drug efflux assay where **compound 5** application resulted in lowered calcein AM retention, hence increased drug efflux.

3. Discussion

Despite improvements in the early detection and following treatment approaches, breast cancer remains a major health issue in both developed and developing countries. This is partly the consequence of the disorganization of multiple signaling mechanisms such as apoptotic pathways. Additionally, acquired MDR following chemotherapy constitutes another obstacle against successful treatment [25]. That being the case, the pursuit of novel agents to inhibit the proliferation of breast cancer cells without causing drug resistance is of interest of the recent studies [26,27]. Being responsible for the leading cause of death among women worldwide, breast cancer has different subtypes with various genetic, morphologic, and histopathologic features. The immune-histological markers and pathological variables help to diagnose the subtype to treat the disease meticulously [28].

Wild-type p53 is a transcription factor and tumor suppressor protein that is encoded by the TP53 gene. p53 protein strictly controls plenty of cellular processes such as cell cycle regulation and DNA repair mechanisms. Under normal conditions, the p53 level is maintained depressed by Mdm2 protein through proteasomal degradation. In the case of acute stress like DNA damage, oncogene activation, hypoxia, ribosome, and/or endoplasmic reticulum stress; Mdm2 is inactivated. Then, p53 is upregulated to arrest the cell cycle until stress stimuli are eliminated or to initiate the apoptotic pathway when the DNA damage is irreversible [29–36]. Several proteins (BAX, BID, PUMA, NOXA, etc.) are induced by p53 which in turn activate caspases to degrade specific regulatory and structural proteins, hence cell death occurs [37]. The interactions between these pro-apoptotic proteins and the survival proteins (BCL-2, BCL-xL, MCL-1, etc.) determine the fate of the cell. Any obstruction to this balance may cause cancer and impinge on the efficacy of cancer treatment [38].

The process of drug discovery and development mandates accurate evaluation of the pharmacokinetic properties of the compounds including absorption, distribution, metabolism, excretion, and toxicity (ADMET) [39]. Unsuitable pharmacokinetic characteristics of a molecule including inadequate absorption, short half-life, rapid clearance, low bioavailability, and high toxicity lead to the failure of a drug candidate to proceed to the next stages of the drug development [40]. Besides, lipophilicity should be considered since it is a critical factor for the passive influx of the compound by the cell through the membrane [41]. The partition coefficient in octanol/water (calculated log P, clog P) value is evaluated as an indicator of the lipophilicity and hence, targeting the efficiency of the drug candidate [42]. It is well known that, compared to the membrane of healthy cells, the tumor cell membrane is comprised of more lipid-enriched microdomains [43]. It is at least partly due to the fast proliferation rate of cancer cells and their requirement of extra supplements such as nutrients and growth factors [44,45]. Thus, a certain level of lipophilicity of the drug candidate may be beneficial to target the cancer cells. Breast cancer cell lines including MCF-7 was proved to possess an elevated content of cholesterol, cholesterol esters, and phospholipids [46,47]. In the present study, the KA analog ALM and its Mannich bases were synthesized by our team, and their cytotoxic effect on the ER and PR-positive MCF-7 and the metastatic triple-negative MDA-MB-231 breast cancer cell lines were inspected. The results showed that **compound 5** hindered cell viability of both MCF-7 (96.95 μM) and MDA-MB-231 (47.79 μM) in a time and dose-dependent manner and has shown a very low harmful effect on HGF-1

healthy cells (410 μM) [19]. Since **compound 5** is lipophilic with a high clog P value; it was hypothesized that the ALM derivative can penetrate through the membrane of breast cancer cell lines via passive transport.

Additionally, the newly synthesized **compound 2**, bearing 4-trifluoromethyl-benzylpiperazine moiety, also showed a remarkable cytotoxic influence on both MCF-7 and MDA-MB-231 cells, where the IC_{50} values for 48 h were calculated to be 105 and 42.48 μM, respectively. However, the morphological observations of both compounds revealed that **compound 5** had a more peculiar effect on both of the cell lines suggesting that distinct cell death mechanisms may be triggered upon administration. Hence, from this point on in this study, **compound 5** was chosen for further detailed exploration.

TNBC cell line MDA-MB-231 bears one allele of mutant TP53 which carries lysine (AAA) instead of arginine (AGA) on codon 280 of exon 8, which is situated on the specific DNA-binding domain and the evolutionarily conserved region [48,49]. Thus, the p53 apoptotic pathway is not triggered in MDA-MB-231 cells in response to many antineoplastic agents [24,50,51]. Accordingly, the findings obtained from this study indicated that **compound 5** provoked necrosis in MDA-MB-231 cells given that the treatment of the cells caused increased LDH activity in cell media meanwhile not stimulating neither the activity of caspases 8 and 9 nor the expression of the pro-apoptotic genes examined. It was concluded that the ALM derivative directed MDA-MB-231 cells to necrosis rather than a highly pre-orchestrated death. Interestingly, a totally different phenomenon was observed in MCF-7 cells indicating apoptosis. The subjection of the cells to **compound 5** did not escalate LDH leakage from the cells although the inhibition of the caspases by Z-VAD-FMK guided the cell towards necrosis proved by the augmented LDH activity in the media. The activity of both caspase 8 and 9 was triggered following the incubation of MCF-7 cells with the derivative molecule, not to mention the pro-apoptotic genes TP53 and Bax were overexpressed whereas the negative regulator TP53, Mdm2, was diminished.

In the literature, the internal ROS level is controversial however, it is known that induced internal H_2O_2 leads most cells to cell death and apoptosis may be stimulated by inhibiting ROS with antioxidants [52,53]. ROS accumulation is considered to cause genomic instability, inhibit caspase activation, and therefore endorse malignancy [54,55]. ROS production due to prolonged usage of chemotherapeutic agents can also initiate survival pathways such as PI3K/Akt, NF-KB, and MDR [56–60]. According to the results, the internal H_2O_2 level was significantly reduced, stating that **compound 5** helped to suppress the internal ROS level of MCF-7 cells. Not so similarly, MDA-MB-231 cells exhibited slightly ascended levels of H_2O_2, a consistent and expected result taken together with previous experiments.

Another obstacle in the treatment of cancer is multidrug resistance which is distinguished by excessive drug efflux from the cells, via the P-glycoprotein (P-gp) situated on the cell membrane. Defeating the function P-gp is the major focus to overcome drug resistance triggered by chemotherapeutical agents, including DOX [61,62]. Therefore, to sum up, to succeed in chemotherapeutical applications, it is highly important to find a molecule that is effective enough to activate cell death without stimulating resistance in cancer cells and having no cytotoxic effect on healthy cells. In this study, we showed that **compound 5** was able to meet the criteria mentioned above in MCF-7 cells by directing the cells toward p53-dependent apoptosis, and by suppressing multidrug resistance at least partially caused by the Mdr-1 gene without harming healthy cells. In MDA-MB-231 cells, the derivative compound acted independently from the p53 pathway, slightly generated oxidative stress that led to cell death, and failed to stimulate the efflux of the agent from the cells, although expression of the Mdr-1 gene was upregulated by 1.4 fold in comparison to the untreated control. Taken together, compared to the conventionally used chemotherapeutics which cause systematic toxicity such as DOX, **compound 5** was shown to cause significant toxicity on both breast cancer cell lines by leading them to cell death without disturbing healthy cells.

4. Conclusion

Overall, in this study, we aspired to explore the anti-proliferative effects of the ALM derivatives in the structure of Mannich bases, on two different breast cancer cell lines for the first time. As observed from the aforementioned experiments based on gene expression studies, it can be concluded that highly lipophilic **compound 5** which is foreseen to penetrate the cell membrane via passive transport could kill breast cancer cells dominantly via a p53-dependent and p53-independent mechanism dependent on the characteristics of the cells. Unlike widely used chemotherapeutics such as DOX, the derivative compound was shown to be relatively harmless to the healthy cell lines since it inhibited proliferation of both of the breast cancer cell lines and it did not trigger drug efflux even in TNBC cell line MDA-MB-231 that is a resistant sub-type of breast cancer by nature. Further tests are in need to enlighten the exact mechanism of action, however, based on the potency of the compound in breast cancer cells, it appears that this compound could be a promising candidate for therapeutic purposes on both ER/PR-possessing and triple-negative breast cancer cells.

5. Experimental

5.1. Chemistry

Entire chemicals used for the synthesis of the ALM derivatives were purchased from Merck (Germany) and Aldrich Chemical Co. (Germany). Melting points were ascertained with the aid of Thomas Hoover Capillary Melting Point Apparatus (USA) and uncorrected. IR spectra were recorded on a Perkin Elmer FT-IR-420 System, Spectrum BX spectrometer. 1H- 13C NMR spectra were attained with a Varian Mercury 400 MHz spectrophotometer in deuterochloroform ($CDCl_3$) and dimethyl sulfoxide (DMSO-d_6). Tetramethylsilane (TMS) was used as an internal standard (chemical shift in d, ppm). Mass spectrometry analysis was achieved with a Micromass ZQ LC-MS with Masslynx Software Version 4.1 by adopting the electrospray ionization (ESI+) method. The elemental analysis was carried out with a Leco CHNS-932 analyzer (Leco, St. Joseph, MI, USA) in the Central Laboratory of Ankara University, Faculty of Pharmacy. The purity of the compounds was investigated by thin-layer chromatography (TLC) on Kieselgel 60 F254 (Merck, Germany) chromatoplates.

5.2. Synthesis of CKA and ALM

CKA and ALM were synthesized by adapting a previous method [8]. CKA: Yield 76%, mp 166–7 °C (lit. 166–7 °C). ALM: Yield 63%, mp 152–3 °C (lit. 152–3 °C).

5.3. Synthesis of Mannich bases (Compounds 1–7)

Mannich bases were produced by the reaction of substituted piperazine derivatives and ALM in MeOH with 37% formalin. The solution was stirred vigorously for 15 to 25 min. The resulting precipitate was collected by filtration and washed with cold MeOH. All crude products were recrystallized with the appropriate solvents. The basic scheme of the synthesis process was displayed in Fig. 1. The characteristics of the ALM and its derivatives were exhibited in Table 1.

2-((4-(4-(Trifluoromethyl)benzyl)piperazin-1-yl)methyl)-3-hydroxy-6-methyl-4H-pyran-4-one (compound 2) $C_{19}H_{21}F_3N_2O_3$ (M.W.: 382.38 g/mol), yield: 71%, mp: 171–2 °C, clog P: 3.013. %CHN Found (Calculated): C 59.30 (59.68), H 5.58 (5.54), N 7.41 (7.33). IR ν (cm^{-1}): 2820 (C—H (aliphatic)), 1621 (C═O), 1453 (C═C), 1321 (C—N), 1198 (C—O). ^{1}H NMR ($CDCl_3$, 400 MHz) δ ppm: 2.26 (3H; s; -CH_3); 2.49 (4H; brs; piperazine); 2.62 (4H; brs; piperazine); 3.53 (2H; s; pyrane-CH_2-piperazine); 3.63 (2H; s; –CH_2-Ar); 6.18 (1H; s; pyrane-H^5); 7.41 (2H; d; Ar- $H^{2',6'}$); 7.53 (2H; d; Ar- $H^{3',5'}$). ^{13}C NMR ($CDCl_3$, 100 MHz) 20.12; 52.82; 55.18; 62.22; 111.31; 120.14; 122.84; 125.14; 128.25; 129.18;

142.25; 145.28; 165.22; 173.97. ESI-MS (*m/z*) 382 (100%, $(M)^+$). HRMS calcd $[(M + H)^+]$ 383.1583, measured $[(M + H)^+]$ 383.1586.

2-((4-(2,6-Dichlorobenzyl)piperazin-1-yl)methyl)-3-hydroxy-6-methyl-4H-pyran-4-one (compound 4) $C_{18}H_{20}Cl_2N_2O_3$ (M.W.: 383.27 g/mol), yield: 60%, mp: 165–6 °C, clog P: 3.436. %CHN Found (Calculated): C 56.22 (56.41), H 5.19 (5.26), N 7.57 (7.31). IR ν (cm^{-1}): 2829 (C—H (aliphatic)), 1618 (C═O), 1435 (C═C), 1196 (C—N), 1002 (C—O). ^{1}H NMR (DMSO, 400 MHz) δ ppm: 2.41 (3H; s; -CH_3); 2.51 (4H; brs; piperazine); 2.51 (4H; m; piperazine); 3.48 (2H; s; pyrane-CH2-piperazine); 3.66 (2H; s; -CH_2-Ar); 6.21 (1H; s; pyrane-H^5); 7.30–7.34 (1H; m; Ar-$H^{4\prime}$); 7.45 (2H; d; Ar- $H^{3\prime,5\prime}$).^{13}C NMR (DMSO, 100 MHz) 19.38; 52.36; 52.50; 53.51; 55.87; 111.16; 128.56; 129.83; 133.62; 136.08; 143.29; 146.52; 164.66; 173.50. ESI-MS (*m/z*) 383 (100%, $(M)^+$); 385 $(M + 2)^+$. HRMS calcd $[(M + H)^+]$ 383.0929, measured $[(M + H)^+]$ 383.0931.

2-((4-(2-Chloro-6-fluorobenzyl)piperazin-1-yl)methyl)-3-hydroxy-6-methyl-4H-pyran-4-one (compound 6) $C_{18}H_{20}CFN_2O_3$ (M.W.: 366.81 g/mol), yield: 20%, mp: 153–5 °C, clog P: 2.986. %CHN Found (Calculated): C 58.61 (58.94), H 5.73 (5.50), N 7.70 (7.64). IR ν (cm^{-1}): 3222 (O—H), 2938, 2811 (C—H (aliphatic)), 1612 (C═O), 1449 (C═C), 1317 (C—N), 1212 (C—O). ^{1}H NMR (DMSO, 400 MHz) δ ppm: 2.24 (3H; s; -CH_3); 2.43 (4H; brs; piperazine); 2.50 (4H; m; piperazine); 3.47 (2H; s; pyrane-CH_2-piperazine); 3.58 (2H; s; -CH_2-Ar); 6.20 (1H; s; pyrane-H^5); 7.20 (1H; m; Ar-$H^{3\prime}$); 7.31–7.40 (2H; m; Ar-$H^{4\prime,5\prime}$). ^{13}C NMR (DMSO, 100 MHz) 19.29; 51.77; 52.24; 53.39; 111.06; 114.11; 114.33; 123.22; 123.40; 125.41; 125.44; 129.90; 130.00; 135.50; 135.56; 143.18; 146.43; 160.15; 162.61; 164.56; 173.40. ESI-MS (*m/z*) 367 (100%, $(M)^+$). HRMS calcd $[(M + H)^+]$ 367.1225, measured $[(M + H)^+]$ 367.1222.

2-((4-(4-Bromo-2-fluorobenzyl)piperazin-1-yl)methyl)-3-hydroxy-6-methyl-4H-pyran-4-one (compound 7) $C_{18}H_{20}BrFN_2O_3$. ½ CH_3OH (M.W.: 427.29 g/mol), yield: 47%, mp: 180–1 °C, clog P: 3.136. %CHN Found (Calculated): C 51.84 (52.00), H 5.05 (5.19), N 7.00 (6.56). IR ν (cm^{-1}): 2818 (C—H (aliphatic)), 1626 (C═O), 1460 (C═C), 1233 (C—N), 999 (C—O). ^{1}H NMR (DMSO, 400 MHz) δ ppm: 2.24 (3H; s; -CH_3); 2.39 (4H; brs; piperazine); 2.51 (4H; brs; piperazine); 3.32 (2H; s; pyrane-CH_2-piperazine); 3.49 (2H; d; -CH_2-Ar); 6.21 (1H; s; pyrane-H^5); 7.33–7.40 (2H; m; Ar-$H^{5\prime,6\prime}$); 7.48 (1H; d; Ar-$H^{3\prime}$). ^{13}C NMR (DMSO, 100 MHz) 19.29; 52.15; 52.28; 53.44; 53.83; 111.06; 118.27; 118.52; 120.06; 120.16; 124.10; 124.24; 127.22; 127.25; 132.87; 132.92; 143.18; 146.46; 159.30; 161.78; 164.56;173.40. ESI-MS (*m/z*) 411 (100%, $(M)^+$), 413 $(M + 2)^+$. HRMS calcd $[(M)^+]$ 411.0720, measured $[(M)^+]$ 411.0722, $[(M + 2)^+]$ 413.0724.

5.4. Cell lines and culture conditions

MCF-7 (ATCC® HTB-22™) and MDA-MB-231 (ATCC® HTB-26™) breast cancer cell lines were obtained from American Type Culture Collection (ATCC, USA). Cells were cultured in Dulbecco's Modified Eagle Medium (DMEM) supplemented with 10% heat-inactivated fetal bovine serum, 1% 200 mM L-glutamine, 100 U/mL penicillin, and 100 μg/mL streptomycin which were all bought from Gibco (USA). Cells were incubated at 37 °C in a humidified atmosphere of 5% CO_2.

5.5. Cell viability assay

Cytotoxic properties of seven ALM derivatives were evaluated with SRB (Santa Cruz Biotechnology, USA) assay. MCF-7 and MDA-MB-231 cells were seeded in 96-well plates at a concentration of 5×10^3 cells/well. When confluent, cells were exposed to 6.25–150 μM of ALM or its analogs, which were dissolved in sub-toxic volumes of DMSO before treatment. After 24, 48, or 72 h of incubation, cells were fixed to the wells with 10% (w/v) trichloroacetic acid (Sigma Aldrich, USA). After cells were washed with dH_2O, 0.06% (w/v) SRB dye was applied to each well, and incubation at room temperature for 30 min was ensured. Following the incubation, the excess dye was removed from the wells with the application 1% (v/v) acetic acid (Sigma Aldrich, USA). Finally, tris base (10 mM, pH 10.5) (Sigma Aldrich, USA) was added and the optical density (OD) was measured at 510 nm. Cells not treated with the compounds were considered as the negative control and to be 100% viable. The percentage of absorbance values compared to control were assessed to determine the changes in cell viability. The ALM derivative that caused the highest toxicity on cells was chosen to perform the following experiments.

5.6. Evaluation of the stability of ALM derivative

The UV–visible absorption spectrum of the selected ALM derivative was evaluated to determine the wavelength for the maximum absorbance of the molecule and its stability over time. Three time-points (0 h, 24 h, and 48 h) were selected to test whether the derivative would be stable within this time course. The vial of derivative was 20 mM of concentration and kept at 37 °C until the end of the experiment. The optical characteristics were measured between the wavelengths of 230 nm and 890 nm.

5.7. LDH activity assay

The breast cancer cells were seeded into 6-well plates (1×10^5 cells/well). When confluent, cells were subjected to 1% of Triton X-100 (positive control group), or IC_{50} concentration (at 48 h) of the ALM derivative alone or in combination with the caspase inhibitor Z-VAD-FMK (Sigma-Aldrich, USA). The cells that were not treated with an agent was considered as the negative control group. After 6 h-incubation, the media of each group was collected and the LDH activity assay was carried out by using the ab102526 colorimetric LDH assay kit (Abcam, USA) according to the protocol of the manufacturer. The OD values were measured at 450 nm kinetically and the percentage of the cytotoxicity was calculated according to the equation as follows:

$$\%\text{Cytotoxicity} = (\text{A sample} - \text{A negative control})/(\text{A positive control} - \text{A negative control}) \times 100$$

5.8. Determination of H_2O_2 level

ROS levels of the derivative-treated cells were analyzed through the H_2O_2 content released to the media using the colorimetric OxiSelect™ H_2O_2 assay kit (Cell Biolabs Inc., USA). According to the manufacturer's suggestions, cells were seeded into 6-well plates (1×10^5 cells/well). When confluent, cells were received IC_{50} concentration of the specific compound and incubated for 48 h. Next, the medium in each well was collected and centrifuged at 10,000 × g for 5 min at room temperature to get rid of insoluble particles, and the supernatant obtained was regarded as a sample. The standards (0 – 200 μM) and the supernatant of the samples were transferred to a 96-well plate and the working solution comprised of 1:100 xylenol orange, 1:40 sorbitol, and 1:100 AFS reagent was added. The plate was incubated for 30 min at room temperature, OD values were measured at 595 nm and the hydrogen peroxide level of each sample was determined from the standard curve.

5.9. Measurement of the caspase 8 and 9 activity

To examine the activity of caspase 8 and 9 after the treatment of MCF-7 and MDA-MB-231 cells with the compound-of-interest, the cells were seeded into 6-well plates (1×10^5 cells/well) and incubated until they reach 70% confluency. The cells were subjected to IC_{50} concentration of the ALM derivative for 48 h and the activity levels of the caspases were investigated by employing the ab39700 colorimetric caspase 8 and ab65608 caspase 9 assay kits (both purchased from Abcam, USA) according to the specifications of the kit. The protein concentration was measured using the BCA protein assay kit (Thermo Fischer Scientific, USA) and normalized for each sample. The caspase 8

activity was assessed based on the principle of the enzyme cleaving its specific substrate, the Ile-Glu-Thr-Asp (IETD)-p-nitroanilide, and caspase 9 activity was determined by quantifying the ratio of the cleavage of Leu-Glu-His-Asp (LEHD)-p-nitroanilide by the enzyme. The absorbance for each enzyme was measured at 400 nm and compared to the control to evaluate the relative enzymatic activity ratio.

5.10. Drug efflux assay

The attribution of the novel compound to stimulate MDR in MCF-7 and MDA-MB-231 cells were investigated by using the Vybrant® multidrug resistance assay kit (Thermo Fischer, ABD). Briefly, IC_{50} values of the compound were applied to MCF-7 and MDA-MB-231 cells in 96-well plates (initial concentration of 5×10^3 cells/well). Following 48 h of incubation, cells were treated with calcein acetoxymethyl ester (AM) at a final concentration to be 0.25 μM for 30 min at 37 °C. Calcein AM is known to be not fluorescent yet when it penetrates the cell, it is converted to calcein by endogen esterases which are steeply fluorescent [63]. In this manner, the fluorescence signal will be higher if drug resistance is low in contrast to the low signal when drug resistance is present. The formation of the calcein was judged after measurement at λex of 485 nm and the λem of 520 nm using FLUOstar® Omega plate reader (BMG LabTech, Germany).

5.11. Investigation of gene expression levels

Total RNA was isolated from the compound-treated cells employing the NucleoSpin® RNA isolation kit (Macherey-Nagel, Germany). RNA samples were used as templates for cDNA synthesis achieved with the cDNA synthesis kit (New England BioLabs, USA). cDNA samples were then handled to investigate expressions of TP53, Mdm2, Bax, Bcl-2 apoptotic pathway genes, Mdr-1 gene which ultimately expresses P-gp, an important ABC transporter protein, and GAPDH as the reference housekeeping gene. Primers for TP53 (forward: CACCATGAGCGCTGCC TCA GATAGC, reverse: ACAGGCACAAACACGCACCTCAAA), Mdm2 (forward: AGGTCACTC CGATGAAAGGT, reverse: GTTGTCTAGTAC-CATTAACC), Bax (forward: TTTCATCCAG GATCGAGCAG, reverse: AAAGTAGAAAAGGGCGACAA), Bcl-2 (forward: GTGTGTG GAGA GCGTCAACCGG, reverse: TCAAACAGAGGCCGCATGCTGG), Mdr-1 (forward: TTCAACTATCCCACCCGACCGGAC, reverse: ATGCTGCAGT-CAAACAGGATGGGC), and GAPDH (forward: GTCGTATTG GGCGCCTGGTCAC, reverse: GCCAGCATCGCCCCAC TTGATT) were designed taking into account of National Center for Biotechnology Information (NCBI). Gene expression levels were measured utilizing SYBR green master mix (Thermo Fischer, USA) by Applied Biosystems ViiA™ 7 (USA) device. The qRT-PCR conditions were as follows: 95 °C for 10 min, followed by 40 cycles of 95 °C for 15 *sec* and 60 °C for 1 min. The relative alterations in the transcriptional levels of the genes between the untreated cells and cells treated with IC_{50} concentration of the compound were measured using the comparative Ct method ($2^{-\Delta\Delta Ct}$).

5.12. Statistical analysis

All tests were conducted to be at least three replicates (n = 3). Differences between groups were analyzed with a two-sided paired or unpaired *t*-test by use of GraphPad Prism 5.3 software. Results were considered to be statistically significant when $p < 0.05$.

Declaration of Competing Interest

The authors declare that they have no known competing financial interests or personal relationships that could have appeared to influence the work reported in this paper.

Acknowledgment

The authors wish to thank Hacettepe University Scientific Research Projects Coordination Unit for financial support of this study (Project ID: THD-2016-11528) and the Central Laboratory of Ankara University Faculty of Pharmacy for providing the instrumental facility used in this work.

Appendix A. Supplementary material

Supplementary data to this article can be found online at https://doi.org/10.1016/j.bioorg.2020.104403.

References

[1] Q.K. Song, X.L. Wang, X.N. Zhou, H.B. Yang, Y.C. Li, J.P. Wu, J. Ren, H.K. Lyerly, Breast cancer challenges and screening in china: lessons from current registry data and population screening studies, Oncologist 20 (2015) 773–779.
[2] D.L. Holliday, V. Speirs, Choosing the right cell line for breast cancer research, Breast Cancer Res. 13 (2011) 215.
[3] J.M. Ford, W.N. Hait, Pharmacology of drugs that alter multidrug resistance in cancer, Pharmacol. Rev. 42 (1990) 155–199.
[4] L. Zinzi, E. Capparelli, M. Cantore, M. Contino, M. Leopoldo, N.A. Colabufo, Small and innovative molecules as new strategy to revert MDR, Front. Oncol. 4 (2014) 2.
[5] B.-W. Liu, P.-C. Huang, J.-F. Li, F.-Y. Wu, Colorimetric detection of tyrosinase during the synthesis of kojic acid/silver nanoparticles under illumination, Sens. Actuators, B 251 (2017) 836–841.
[6] R. Saruno, F. Kato, T. Ikeno, Kojic acid, a tyrosinase inhibitor from Aspergillus albus, Agric. Biol. Chem. 43 (1979) 1337–1338.
[7] M. Aytemir, B. Ozcelik, I.E. Orhan, G. Karakaya, F.S. Senol, Kojic acid-derived mannich bases with biological effect, Google Patents (2018).
[8] M.D. Aytemir, G. Karakaya, Kojic acid derivatives, D. Ekinci (Ed.), Medicinal Chemistry and Drug Design, Intech Open, Rijeka, 2012, pp. 1-26.
[9] J. Chaudhary, S. Lakhawat, A.N. Pathak, Elucidation on enhanced application of synthesised kojic acid immobilised magnetic and chitosan tri-polyphosphate nanoparticles as antibacterial agents, IET Nanobiotechnol. 9 (2015) 375–380.
[10] J.-F. Hsieh, S.-T. Chen, S.-L. Cheng, Molecular Profiling of A375 Human Malignant Melanoma Cells Treated with Kojic Acid and Arbutin, Y. Tanaka (Ed.) Breakthroughs in Melanoma Research, InTech Open, 2011, pp. 533-558.
[11] S.M. Ahn, H.S. Rho, H.S. Baek, Y.H. Joo, Y.D. Hong, S.S. Shin, Y.H. Park, S.N. Park, Inhibitory activity of novel kojic acid derivative containing trolox moiety on melanogenesis, Bioorg. Med. Chem. Lett. 21 (2011) 7466–7469.
[12] M.D. Atemir, B. Özçelik, Synthesis and biological activities of new Mannich bases of chlorokojic acid derivatives, Med. Chem. Res. 20 (2011) 443–452.
[13] M.D. Aytemir, B. Ozcelik, G. Karakaya, Evaluation of bioactivities of chlorokojic acid derivatives against dermatophytes couplet with cytotoxicity, Bioorg. Med. Chem. Lett. 23 (2013) 3646–3649.
[14] G. Karakaya, M.D. Aytemir, B. Ozcelik, U. Calis, Design, synthesis and in vivo/in vitro screening of novel chlorokojic acid derivatives, J. Enzyme Inhib. Med. Chem. 28 (2013) 627–638.
[15] G. Karakaya, A. Ercan, S. Öncül, M.D. Aytemir, Kojic acid derivatives as potential anticancer agents: Synthesis and cytotoxic evaluation on A375 human malignant melanoma cells, J. Res. Pharm. 23 (2019) 596–607.
[16] É.A. Enyedy, O. Dömötör, E. Varga, T. Kiss, R. Trondl, C.G. Hartinger, B.K. Keppler, Comparative solution equilibrium studies of anticancer gallium (III) complexes of 8-hydroxyquinoline and hydroxy (thio) pyrone ligands, J. Inorg. Biochem. 117 (2012) 189–197.
[17] K. Saatchi, K.H. Thompson, B.O. Patrick, M. Pink, V.G. Yuen, J.H. McNeill, C. Orvig, Coordination chemistry and insulin-enhancing behavior of vanadium complexes with maltol C6H6O3 structural isomers, Inorg. Chem. 44 (2005) 2689–2697.
[18] W. Kandioller, A. Kurzwernhart, M. Hanif, S.M. Meier, H. Henke, B.K. Keppler, C. G. Hartinger, Pyrone derivatives and metals: From natural products to metal-based drugs, J. Organometal Chem. 696 (2011) 999–1010.
[19] G. Karakaya, A. Ercan, S. Oncul, M.D. Aytemir, Synthesis and cytotoxic evaluation of kojic acid derivatives with inhibitory activity on melanogenesis in human melanoma cells, Anti-Cancer Agents Med. Chem. 18 (2018) 2137–2148.
[20] G. Karakaya, A. Türe, A. Ercan, S. Oncul, M.D. Aytemir, Synthesis, computational molecular docking analysis and effectiveness on tyrosinase inhibition of kojic acid derivatives, Bioorg. Chem. (2019), 102950.
[21] I. Ichimoto, H. Ueda, C. Tatsumi, K. Fujii, F. Sekido, S. Nonomura, Studies on kojic acid and its related γ-pyrone compounds: Part VII. The alkylation of kojic acid and pyromeconic acid through their mannich base (Synthesis of maltol-(1)) Part VIII. Synthesis of comenic acid from kojic acid (Synthesis of maltol (2)), Agric. Biol. Chem. 29 (1965) 94–103.
[22] F. Yang, S.S. Teves, C.J. Kemp, S. Henikoff, Doxorubicin, DNA torsion, and chromatin dynamics, BBA 2014 (1845) 84–89.
[23] E.R. Hayek, E. Speakman, E. Rehmus, Acute doxorubicin cardiotoxicity, New Eng. J. Med. 352 (2005) 2456–2457.
[24] S. Oncul, A. Ercan, Discrimination of the effects of doxorubicin on two different breast cancer cell lines on account of multidrug resistance and apoptosis, Ind. J. Pharm. Sci. 79 (2017).

[25] R. Saxena, G. Gupta, M. Manohar, U. Debnath, P. Popli, Y.S. Prabhakar, R. Konwar, S. Kumar, A. Kumar, A. Dwivedi, Spiro-oxindole derivative 5-chloro-4',5'-diphenyl-3'-(4-(2-(piperidin-1-yl) ethoxy) benzoyl) spiro[indoline-3,2'-pyrrolidin]-2-one triggers apoptosis in breast cancer cells via restoration of p53 function, Int. J. Biochem. Cell Biol. 70 (2016) 105–117.
[26] P. Gilson, F. Josa-Prado, C. Beauvineau, D. Naud-Martin, L. Vanwonterghem, F. Mahuteau-Betzer, A. Moreno, P. Falson, L. Lafanechere, V. Frachet, J.L. Coll, J. Fernando Diaz, A. Hurbin, B. Busser, Identification of pyrrolopyrimidine derivative PP-13 as a novel microtubule-destabilizing agent with promising anticancer properties, Sci. Rep. 7 (2017) 10209.
[27] N. Takegawa, Y. Nonagase, K. Yonesaka, K. Sakai, O. Maenishi, Y. Ogitani, T. Tamura, K. Nishio, K. Nakagawa, J. Tsurutani, DS-8201a, a new HER2-targeting antibody-drug conjugate incorporating a novel DNA topoisomerase I inhibitor, overcomes HER2-positive gastric cancer T-DM1 resistance, Int. J. Cancer 141 (2017) 1682–1689.
[28] A.H. Sims, A. Howell, S.J. Howell, R.B. Clarke, Origins of breast cancer subtypes and therapeutic implications, Nat. Clin. Pract. Oncol. 4 (2007) 516–525.
[29] H. Brito, A.C. Martins, J. Lavrado, E. Mendes, A.P. Francisco, S.A. Santos, S. A. Ohnmacht, N.S. Kim, C.M. Rodrigues, R. Moreira, S. Neidle, P.M. Borralho, A. Paulo, Targeting KRAS oncogene in colon cancer cells with 7-carboxylate indolo [3,2-b]quinoline tri-alkylamine derivatives, PLoS ONE 10 (2015) e0126891.
[30] H.A. Ceja-Rangel, P. Sanchez-Suarez, E. Castellanos-Juarez, R. Penaroja-Flores, D. J. Arenas-Aranda, P. Gariglio, L. Benitez-Bribiesca, Shorter telomeres and high telomerase activity correlate with a highly aggressive phenotype in breast cancer cell lines, Tumour Biol. 37 (2016) 11917–11926.
[31] H.T. Wang, T.Y. Chen, C.W. Weng, C.H. Yang, M.S. Tang, Acrolein preferentially damages nucleolus eliciting ribosomal stress and apoptosis in human cancer cells, Oncotarget 7 (2016) 80450–80464.
[32] R. Jakhar, S. Paul, M. Bhardwaj, S.C. Kang, Astemizole-Histamine induces Beclin-1-independent autophagy by targeting p53-dependent crosstalk between autophagy and apoptosis, Cancer Lett. 372 (2016) 89–100.
[33] V.E. Ghouzzi, F.T. Bianchi, I. Molineris, B.C. Mounce, G.E. Berto, M. Rak, S. Lebon, L. Aubry, C. Tocco, M. Gai, A.M. Chiotto, F. Sgro, G. Pallavicini, E. Simon-Loriere, S. Passemard, M. Vignuzzi, P. Gressens, F. Di Cunto, ZIKA virus elicits P53 activation and genotoxic stress in human neural progenitors similar to mutations involved in severe forms of genetic microcephaly and p53, Cell Death Dis. 7 (2016) e2440.
[34] B.C. Cheng, J.T. Chen, S.T. Yang, C.C. Chio, S.H. Liu, R.M. Chen, Cobalt chloride treatment induces autophagic apoptosis in human glioma cells via a p53-dependent pathway, Int. J. Oncol. 50 (2017) 964–974.
[35] P. Subash-Babu, D.K. Li, A.A. Alshatwi, In vitro cytotoxic potential of friedelin in human MCF-7 breast cancer cell: Regulate early expression of Cdkn2a and pRb1, neutralize mdm2-p53 amalgamation and functional stabilization of p53, Exp. Toxicol. Pathol. 69 (2017) 630–636.
[36] L. Hauck, S. Stanley-Hasnain, A. Fung, D. Grothe, V. Rao, T.W. Mak, F. Billia, Cardiac-specific ablation of the E3 ubiquitin ligase Mdm2 leads to oxidative stress, broad mitochondrial deficiency and early death, PLoS ONE 12 (2017) e0189861.
[37] L.N. Zhang, J.Y. Li, W. Xu, A review of the role of Puma, Noxa and Bim in the tumorigenesis, therapy and drug resistance of chronic lymphocytic leukemia, Cancer Gene Ther. 20 (2013) 1–7.
[38] J. Deng, How to unleash mitochondrial apoptotic blockades to kill cancers? Acta Pharm. Sin. B 7 (2017) 18–26.
[39] J.T. Dalton, Pharmacokinetics and Metabolism in Drug Design. Methods and Principles in Medicinal Chemistry. Volume 31. Second Revised Edition By Dennis A. Smith, Han van de Waterbeemd, and Don K. Walker. Wiley-VCH, Weinheim, Germany. 2006. xix + 187 pp. 17.5 × 24.5 cm. ISBN 3527313680. $125.00, J Med Chem, 49 (2006) 7556-7557.
[40] H. Rosen, T. Abribat, The rise and rise of drug delivery, Nat. Rev. Drug Discov. 4 (2005) 381–385.
[41] X. Liu, B. Testa, A. Fahr, Lipophilicity and its relationship with passive drug permeation, Pharm. Res. 28 (2011) 962–977.
[42] E. Milanetti, D. Raimondo, A. Tramontano, Prediction of the permeability of neutral drugs inferred from their solvation properties, Bioinformatics 32 (2016) 1163–1169.
[43] Y.C. Li, M.J. Park, S.-K. Ye, C.-W. Kim, Y.-N. Kim, Elevated levels of cholesterol-rich lipid rafts in cancer cells are correlated with apoptosis sensitivity induced by cholesterol-depleting agents, Am. J. Pathol. 168 (2006) 1107–1118.
[44] V. Lladó, D.J. López, M. Ibarguren, M. Alonso, J.B. Soriano, P.V. Escribá, X. Busquets, Regulation of the cancer cell membrane lipid composition by NaCHOleate: Effects on cell signaling and therapeutical relevance in glioma, Biochim. Biophys. Acta (BBA) – Biomembr. 1838 (2014) 1619–1627.
[45] N. Bernardes, A.M. Fialho, Perturbing the dynamics and organization of cell membrane components: a new paradigm for cancer-targeted therapies, Int. J. Mol. Sci. 19 (2018) 3871.
[46] I.N. Todor, N.Y. Lukyanova, V.F. Chekhun, The lipid content of cisplatin- and doxorubicin-resistant MCF-7 human breast cancer cells, Exp. Oncol. 34 (2012) 97–100.
[47] G. Varan, S. Öncül, A. Ercan, J.M. Benito, C. Ortiz Mellet, E. Bilensoy, Cholesterol-targeted anticancer and apoptotic effects of anionic and polycationic amphiphilic cyclodextrin nanoparticles, J. Pharm. Sci. 105 (2016) 3172–3182.
[48] Y. Li, S. Upadhyay, M. Bhuiyan, F.H. Sarkar, Induction of apoptosis in breast cancer cells MDA-MB-231 by genistein, Oncogene 18 (1999) 3166–3172.
[49] M. Simon, F. Mesmar, L. Helguero, C. Williams, Genome-wide effects of MELK-inhibitor in triple-negative breast cancer cells indicate context-dependent response with p53 as a key determinant, PLoS ONE 12 (2017) e0172832.
[50] L. Hui, Y. Zheng, Y. Yan, J. Bargonetti, D.A. Foster, Mutant p53 in MDA-MB-231 breast cancer cells is stabilized by elevated phospholipase D activity and contributes to survival signals generated by phospholipase D, Oncogene 25 (2006) 7305.
[51] E. Pozo-Guisado, A. Alvarez-Barrientos, S. Mulero-Navarro, B. Santiago-Josefat, P. M. Fernandez-Salguero, The antiproliferative activity of resveratrol results in apoptosis in MCF-7 but not in MDA-MB-231 human breast cancer cells: cell-specific alteration of the cell cycle, Biochem. Pharmacol. 64 (2002) 1375–1386.
[52] Y. Ibuki, M. Akaike, T. Toyooka, T. Mori, T. Nakayama, R. Goto, Hydrogen peroxide is critical for UV-induced apoptosis inhibition, Redox Rep. 11 (2006) 53–60.
[53] H.U. Simon, A. Haj-Yehia, F. Levi-Schaffer, Role of reactive oxygen species (ROS) in apoptosis induction, Apoptosis 5 (2000) 415–418.
[54] K. Prabhakaran, L. Li, J.L. Borowitz, G.E. Isom, Caspase inhibition switches the mode of cell death induced by cyanide by enhancing reactive oxygen species generation and PARP-1 activation, Toxicol. Appl. Pharmacol. 195 (2004) 194–202.
[55] M. Takahashi, M. Higuchi, H. Matsuki, M. Yoshita, T. Ohsawa, M. Oie, M. Fujii, Stress granules inhibit apoptosis by reducing reactive oxygen species production, Mol. Cell. Biol. 33 (2013) 815–829.
[56] J. Hou, A. Cui, P. Song, H. Hua, T. Luo, Y. Jiang, Reactive oxygen species-mediated activation of the Src-epidermal growth factor receptor-Akt signaling cascade prevents bortezomib-induced apoptosis in hepatocellular carcinoma cells, Mol. Med. Rep. 11 (2015) 712–718.
[57] F. Khan, I. Khan, A. Farooqui, I.A. Ansari, Carvacrol induces reactive oxygen species (ROS)-mediated apoptosis along with cell cycle arrest at G0/G1 in human prostate cancer cells, Nutr. Cancer (2017) 1–13.
[58] A. Tebbi, F. Levillayer, G. Jouvion, L. Fiette, G. Soubigou, H. Varet, N. Boudjadja, S. Cairo, K. Hashimoto, A.M. Suzuki, P. Carninci, A. Carissimo, D. di Bernardo, Y. Wei, Deficiency of multidrug resistance 2 contributes to cell transformation through oxidative stress, Carcinogenesis 37 (2016) 39–48.
[59] Y.Y. Wu, J.H. Zhang, J.H. Gao, Y.S. Li, Aloe-emodin (AE) nanoparticles suppresses proliferation and induces apoptosis in human lung squamous carcinoma via ROS generation in vitro and in vivo, Biochem. Biophys. Res. Commun. 490 (2017) 601–607.
[60] L. Yuan, S. Wei, J. Wang, X. Liu, Isoorientin induces apoptosis and autophagy simultaneously by reactive oxygen species (ROS)-related p53, PI3K/Akt, JNK, and p38 signaling pathways in HepG2 cancer cells, J. Agric. Food Chem. 62 (2014) 5390–5400.
[61] M. Calvani, A. Dabraio, G. Bruno, V. De Gregorio, M. Coronnello, C. Bogani, S. Ciullini, G. Marca, M. Vignoli, P. Chiarugi, M. Nardi, A.M. Vannucchi, L. Filippi, C. Favre, β3-Adrenoreceptor blockade reduces hypoxic myeloid leukemic cells survival and chemoresistance, Int. J. Mol. Sci. 21 (2020).
[62] C.C. Hung, C.Y. Chen, Y.C. Wu, C.F. Huang, Y.C. Huang, Y.C. Chen, C.S. Chang, Synthesis and biological evaluation of thiophenylbenzofuran derivatives as potential P-glycoprotein inhibitors, Eur. J. Med. Chem. 201 (2020), 112422.
[63] F.L. Miles, J.E. Lynch, R.A. Sikes, Cell-based assays using calcein acetoxymethyl ester show variation in fluorescence with treatment conditions, J. Biol. Methods 2 (2015) e29.